

Multiphase Hydrocarbons from Carboniferous Reservoir Rocks and Their Origin in the Donghetang Area, Western Tabei Uplift, Tarim Basin, NW China

Zhicheng Lei ^{a,b,c}, Huaimin Xu ^a, , Tongwen Jiang ^d, Zhongchao Li ^b, Jingwen Li ^a, Weilu Li ^e, Yunbin Xiong ^b, Songze Li ^{b,c}, Junwei Zhao ^a

^aDepartment of Geoscience, China University of Petroleum-Beijing, Beijing 102249, China

^bResearch Institute of Petroleum Exploration and Development, Zhongyuan Oilfield Company, Sinopec, Puang, Henan, 457300, China

^cPost-Doctor Research Center, Zhongyuan Oilfield Company, Sinopec, Puyang, Henan, 457300, China

^dResearch Institute of Petroleum Exploration and Development, Tarim Oilfield Company, PetroChina, Korla 841000, China

^eNational Marine Data and Information Service, Tianjing 30071, China

Received 19 November 2017; accepted 1 March 2018

Abstract—The Carboniferous Donghe sandstone reservoir is the most important target in the Tabei Uplift of the Tarim Basin, which contains a range of hydrocarbon types, including bitumen, heavy oil, condensate oil, light oil, crude oil, and hydrocarbon gas, and has high contents of CO₂ and N₂. The origin of multiple phase hydrocarbons from Carboniferous reservoir rocks in the Donghetang area, Western Tabei Uplift, is documented in this paper based on integral analysis of the geochemistry, pyrolysis, and carbon isotopes of the bulk composition and light composition hydrocarbons. Oil–source correlations determined that the paleoreservoir hydrocarbons that formed from Permian to Triassic derived from the Lower Ordovician (O₁) source rocks and that those of the present-day reservoir that formed in the Neogene derived from Middle–Upper Ordovician (O_{2,3}) source rocks. During the uplift episode lasting from Permian to Triassic, the hydrocarbons in the entire paleoreservoir underwent water washing, biodegradation, and bacterial sulfate reduction (BSR), resulting in residual bitumen, heavy oil, H₂S, and pyrites in the paleoreservoir. The high CO₂ and N₂ contents originated from volcanic degassing due to volcanic activity from Permian to Early Triassic. The present-day reservoirs underwent gas washing and evaporative fractionation due to natural gas charging that originated from oil cracking and kerogen degradation in the deeper reservoirs; this resulted in fractionation and formed condensate oil and light oil with a high wax content in the residual crude oil. Based on this research, it was concluded that the diverse hydrocarbon phases in the Donghetang area were primarily attributed to water washing, biodegradation, BSR, volcanic degassing, gas washing, and evaporative fractionation.

Keywords: Multiple phase hydrocarbons, water washing, biodegradation, bacterial sulfate reduction, gas washing, evaporative fractionation, volcanic degassing, Tarim Basin

INTRODUCTION

The physical properties of trapped hydrocarbon accumulations can change due to secondary alteration, such as deasphalting during gas washing (Meulbroek et al., 1998; Losh et al., 2002; Zhu et al., 2013a,b), evaporative fractionation (Thompson, 1987, 1988; Matyasik et al., 2000; Masterson et al., 2001), water washing and biodegradation (Lafargue and Barker, 1988; Wang et al., 2016), and bacterial sulfate reduction (BSR) (Means and Hubbard, 1987). Gas washing occurs when gas hydrocarbon migrates through hydrocarbon reservoirs and dissolves and transports the light hydrocarbon components of the reservoirs to form gas condensates, causing the hydrocarbon components of the original reservoir to differentiate and the residual reservoir becomes enriched in heavy hydrocarbon compounds (Meulbroek et al., 1998; Zhang, 2000); this occurs in many oilfields around

the world (Thompson, 1987, 1988; Dzou and Hughes, 1993; Meulbroek et al., 1998). Water washing and biodegradation thicken the crude oil (Tian et al., 2012). Evaporative fractionation occurs in a reservoir containing two-phase gas-oil hydrocarbons caused by natural gas charging to the reservoir, and the reservoir fluids fractionate due to a change in pressure and temperature during migration (Price et al., 1983; Thompson, 1987, 1988). The light hydrocarbons originating from the fractionation migrate along carrier systems to shallower traps and accumulate to form gas condensates, resulting in the residual reservoir after fractionation containing a different content of heavy hydrocarbon components depending on the fractionation strength (Curiale et al., 1996). Zhang et al. (2002a,b) proposed that the high waxy contents of Ordovician marine oil in the Tabei Uplift, Tarim Basin, formed by evaporative fractionation. BSR can reduce the high-prices sulfur to H₂S, and asphaltene is formed due to hydrocarbon alteration and the associated pyrite and other heavy minerals (Means and Hubbard, 1987; Jia et al., 2015).

 Corresponding author.

E-mail address: oasis_1997@163.com (Huaimin Xu)

The Carboniferous marine Donghe sandstone is one of the most important exploration targets in the Tabei Uplift, Tarim Basin. Multiple tectonic movements and multiple hydrocarbon charging, accumulation and adjustment events resulted in complex hydrocarbon phases containing bitumen, heavy oil, crude oil, light oil and natural gas. There are two hypotheses on the hydrocarbon source rocks of the Donghe sandstone reservoirs in the Tarim Basin; some proposed that the marine hydrocarbon, including the Donghe sandstone reservoirs, originated from Middle-to-Upper Ordovician source rocks (O_{2-3}) (Zhu et al., 2013b; Cheng et al., 2016), and others argued that the Donghe sandstone reservoir hydrocarbons were mixed from Cambrian and Lower Ordovician ($C-O_1$) source rocks. Others proposed that the Halahtang sag marine hydrocarbons in the Tabei Uplift were primarily derived from $C-O_1$ source rocks, instead of O_{2-3} source rocks (Li et al., 2016b). Additionally, some proposed that the Donghe sandstone reservoirs primarily formed during the Permian-to-Triassic accumulation (Zhang et al.,

2012), and some argued that the Donghe sandstone reservoirs primarily formed in the Neogene (Zhang et al., 2011).

This paper provides solutions to the hydrocarbon and genetic origin of different hydrocarbons through the integral analysis of geochemical composition, which can also be a reference of hydrocarbon origin and reservoir formation for other marine reservoirs in the Tarim Basin.

GEOLOGICAL SETTING

The Tarim Basin lies between the Chinese Tianshan Mountains to the north and western Kunlun Mountains to the south and is confined by the Altun Mountains to the southeast (Fig. 1a, b). The Tabei Uplift is located between the Kuche and Manjiaer depression in the Tarim Basin. The Donghetang tectonic belt is located at the northern Halahtang sag, in the central Tabei Uplift (Fig. 1c). It consists of five Carboniferous Donghe sandstone reservoirs (Fig. 1d)

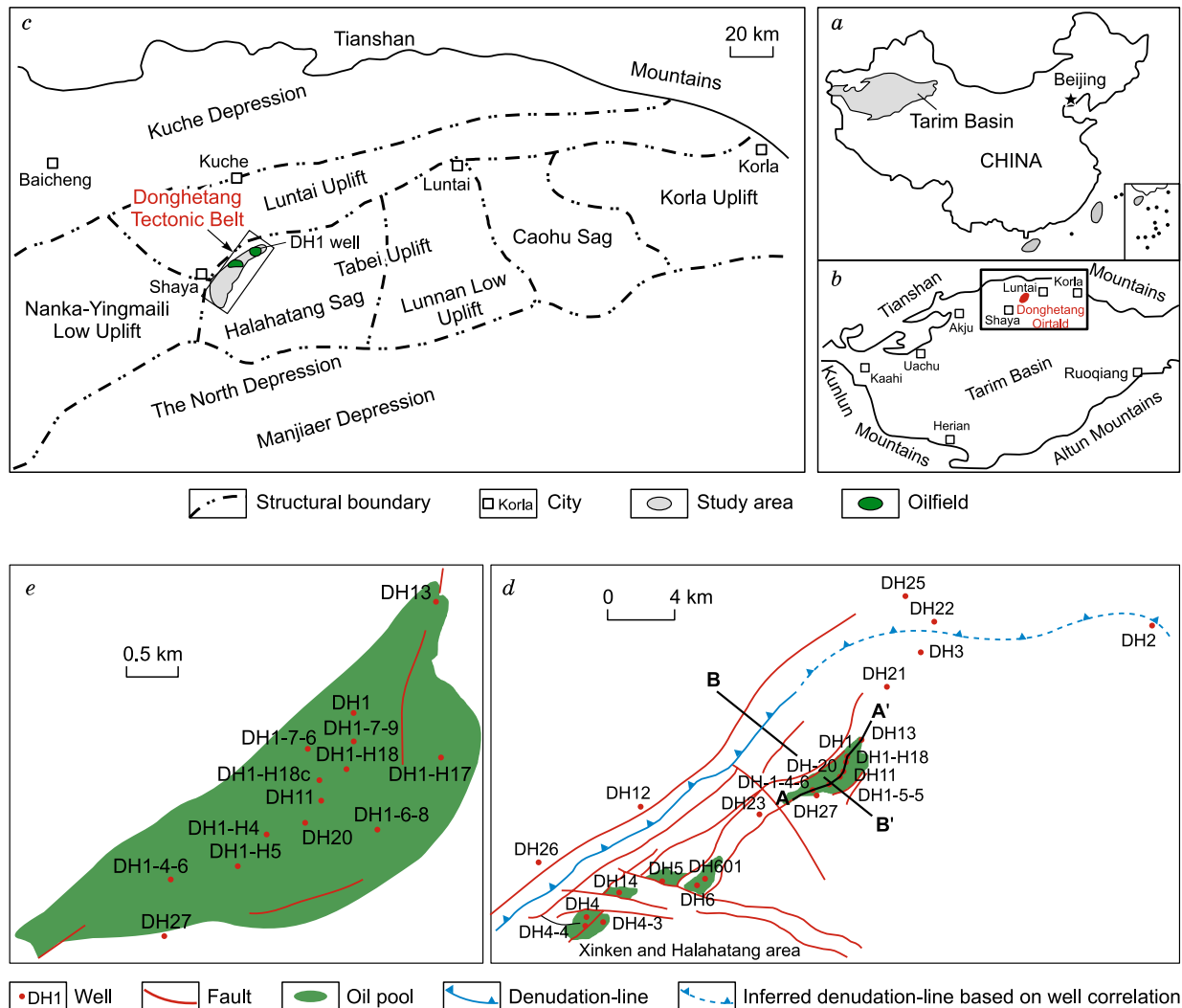


Fig. 1. Tectonic locations of the Tarim Basin (a), Tabei Uplift (b) and Donghetang area (c), respectively; d, fault system and reservoir distribution of the Carboniferous Donghe sandstone in the Donghetang area; e, the well locations in the DH1 Oilfield.

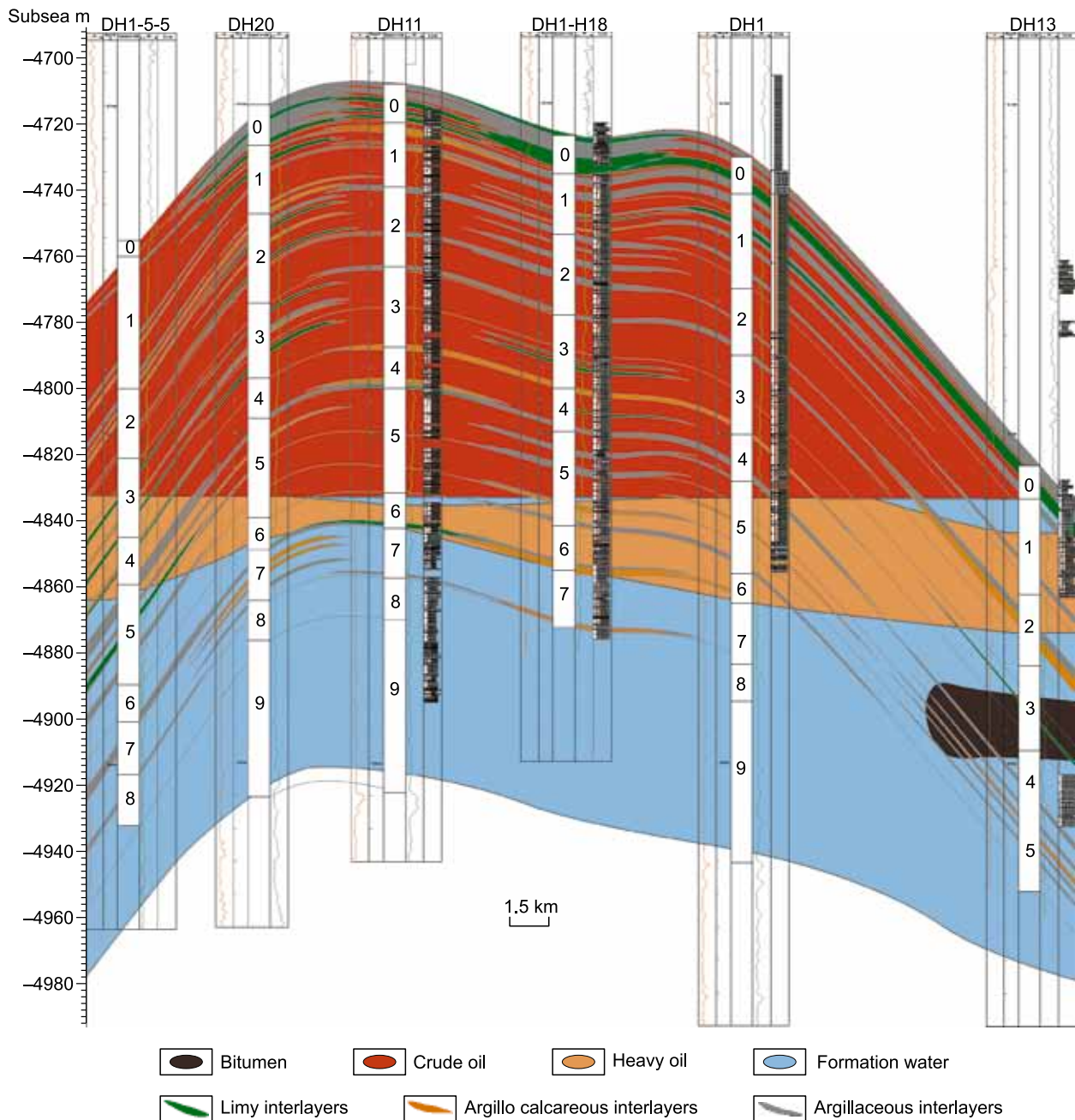


Fig. 2. Cross section of the Carboniferous Donghe sandstone reservoir in the DH1 Oilfield from southwest to northeast. The well locations are shown in Fig. 1d.

and a Jurassic condensate reservoir. There is a uniform oil-water contact (OWC) in the DH1 Oilfield, which is the largest Oilfield in the study area, and the OWC is at -4833 m below sea level (Fig. 2). There is a thick heavy oil zone between 10 to 20 m below the OWC.

The fault system in the study area of the Carboniferous Donghe sandstone is a thrust and strike-slip fault system. The thrust faults strike in a NE–SW direction and the strike-slip faults are dextral and strike in a NW–SE direction (Fig. 1d). The Ordovician to Quaternary strata were drilled in

the study area. Figure 3 shows the sedimentary depositional process and the stratigraphic framework in the study area.

The Donghe sandstone sediments in the study area were deposited on a marine shoreline and are composed of thick fine-grained quartz sandstone (Li et al., 2016a). The Donghe sandstone average thickness is approximately 250 m in the study area and can be divided into 10 sand intervals. Hydrocarbon source rocks in the study area are Ordovician marine carbonate rocks from the southern Manjiaer Depression (Zhang et al., 2000; Chang et al., 2013). The bioclastic lime-

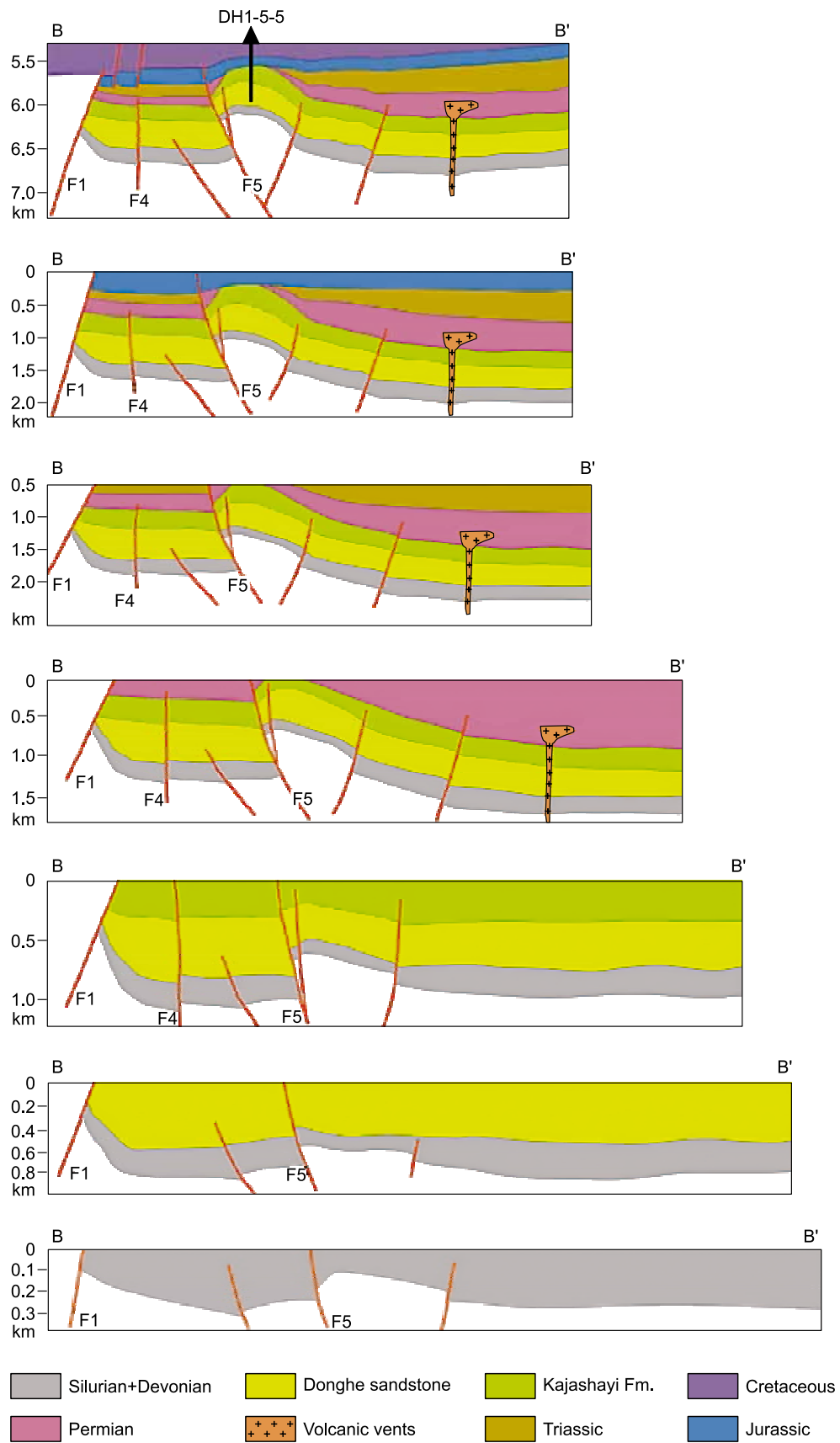


Fig. 3. The structural evolution of the Line B–B'. The profile location and fault numbers are shown in Fig. 1d.

stone and mudstone above the Donghe sandstone are the cap rocks for the Donghe sandstone reservoirs.

Generally, during the Devonian to the Triassic there was an intense thrust and uplift stage and fault activity reached the maximum during the Permian to the Triassic, which is why Permian and Triassic strata were eroded. The study area began to subside in the Jurassic, which resulted in a regional high angle unconformity between the Jurassic and older strata. There was weak thrust activity during the Jurassic to the Cretaceous. The thrust faults in the Paleozoic were reactivated due to negative inversion during the Eocene to Miocene (Li et al., 1998; Tang et al., 1999; Cheng et al., 2009). During this final stage, the strata inclination in the study area experienced inversion due to the subsidence of the northern Kuche Depression, which resulted in a structural high that migrated from north to south, affecting the Jurassic and its overlying strata (Fig. 3).

DATA AND METHODS

The sample suite for this study consists of 15 oil samples, 4 oil sands, 8 top gas samples and 180 meters of reservoir rock samples from the Donghetang Oilfield. A series of geochemical analyses were performed on all the oil samples, including saturated hydrocarbon gas chromatography and light hydrocarbon gas chromatography (GC), which determine the *n*-alkanes distribution, unidentified complex material (UCM) and light hydrocarbon composition. The oil and oil sand samples were geochemically analyzed to determine the physical properties and bulk composition. Rock-eval pyrolysis and carbon isotopic analyses were performed on the samples to determine the pyrolysis parameters and the bulk composition using a sample density of 5 pieces per meter for the DH11 well from the 180 meter-long reservoir.

Gas compositions were measured using an Agilent 7890 gas composition instrument, which was equipped with four valves, six packed columns, a flame ionization detector (FID) and two thermal conductivity detectors (TCD). The oven temperature was held at 50 °C, and the FID temperature remained at 80 °C.

The GC was performed using an Agilent 6890A gas chromatograph equipped with a fused silica column (HP-

PONA, 50 m × 0.20 mm, i.d. × 0.5 mm film thickness) and an FID at 300 °C. The experimental methods of the GC were described in detail by Song et al. (2016). The urea complexation method was used to separate the *n*-alkane and UCM from the oil-saturated hydrocarbons.

The carbon isotopic analyses of the bulk composition: the oil was extracted by washing the oil sand with chloroform, and the bulk composition including alkane, asphaltenes, aromatic and resin was separated using silica gel column chromatography, and the carbon isotopes of each composition was measured using a Finnigan Delta Plus XL isotope ratio mass spectrometer (IRMS); the IRMS experimental methods were described in detail by Guo et al. (2016). The stable carbon isotope data are reported in the δ -notation relative to the PDB standard, and each of the samples was tested at least two times to ensure that the difference between the two measured values was within 0.2‰, and the data reported in this paper are the average of the two measured values.

The rock-eval pyrolysis was performed using a DH-3000 pyrolysis instrument, which was equipped with two valves, a packed column, an FID for monitoring the hydrocarbons contents, three TCDs, and hydrogen as a pyrolysis carrier gas. Initially, a sample is heated at 90 °C for 3 minutes to generate the rock-eval S_0 peak representing the gaseous hydrocarbons contained in the sample; then, it is heated at 300 °C for 3 minutes to generate the rock-eval S_1 peak representing the volatile and semi-volatile hydrocarbons present in the sample. Following this isothermally heated step, the sample is heated linearly from 300 to 600 °C at a rate of 25 °C/min for one minute, yielding the S_2 peak that represents the thermal decomposition products from solid organic matter.

RESULTS

Vertical distribution of hydrocarbon. The Donghe sandstone reservoir is a bottom water massive reservoir with an uneven thickness of heavy oil between the bottom water and crude oil (Fig. 2). From the bottom to the top, the units include: the formation water, heavy oil zone, crude oil and natural gas cap. The reservoir is characterized by high CO₂

Table 1. Natural gas properties of the Carboniferous Donghe sandstone in the study area

Well	Depth, m	Sand interval	Hydrocarbon gas, %	CO ₂ , %	N ₂ , %	Relative density
DH1	5726–5746	2	58.57	18.23	21.61	1.066
	5756–5800	3,4,5	59.38	19.35	20.98	1.009
DH11	5712–5724	1	49.29	26.76	23.95	0.805
DH6	5985–5998	0,1	48.92	23.21	27.87	1.18
DH14	6116–6126	0,1	42.02	22.57	35.41	1.2
DH4	6068–6086	0,1	48.83	20.38	30.64	1.22
DH1-5-5	5745–5795	1,2	53.46	22.24	24.3	0.98
DH1-H18c	5981–6016	2	42.2	31.1	26.6	1.049

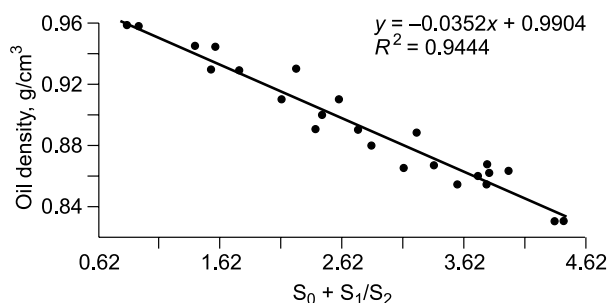


Fig. 4. The relationship between oil density and the pyrolysis parameters for the DH11 well. S_0 , Gaseous hydrocarbon storage in the unit reservoir rock, which primarily represents the light hydrocarbon contents with a carbon chain range from C_1 to C_7 ; S_1 , Liquid hydrocarbon storage in the unit reservoir rock, which represents the free hydrocarbon contents with a carbon chain range from C_8 to C_{33} ; S_2 , Cracking content of the heavy hydrocarbon, resins and asphaltenes that are stored in the reservoir rock with a carbon chain above C_{33} .

and N_2 contents from 18 to 32% and 20 to 36%, respectively (Table 1). There was a strong H_2S odor when the DH11 cores were removed from the barrel in ten sections according to the original core description at the depth of 5730 to 5750 m. There are high pyrite contents that range from 0.1 to 2% in the oil-bearing section and near the oil-water interface, which disagrees with the sediment background. Authigenic massive condensation pyrite crystals occur locally according to the core description.

The oil density was calculated according to the relationship between oil density and the pyrolysis parameters on the

cored section of well DH11 (Figs. 4 and 5). An oil density range of 0.6 to 0.95 g/cm^3 occurs in the hydrocarbon column, which indicates that light oil (0.8–0.84 g/cm^3), condensate oil (<0.8 g/cm^3), heavy oil (>0.9 g/cm^3), crude oil (0.84–0.91 g/cm^3) exist in the reservoir (Fig. 5). The oil density is lighter in the sand intervals of 2 to 3 and heavier in the other sand intervals in the DH11 well hydrocarbon column. Additionally, heavy oil is distributed over the entire hydrocarbon column in the DH11 well.

Physical properties and carbon isotopic analyses for the bulk composition. The crude oil density ranges from 0.84 to 0.885 g/cm^3 , and the viscosity is between 4.1 and 15.2 $mPa \cdot s$. The crude oil wax content is high compared to that of the marine oil, which ranges from 4.6 to 11.9%. The sulfur and saturated hydrocarbon contents range from 0.3 to 0.9% and 38 to 66%, respectively. The asphaltenes content varies significantly, ranging from 4.4 to 47.5%.

The $\delta^{13}C$ values of the rock extract bulk components from the DH11 well are between -32% and -30% . Using the alkane $\delta^{13}C$ values as an example, the DH11 well components can be divided into four sections: the top well sections between 5702 and 5725 m are composed of a light isotope segment, in which the $\delta^{13}C$ values range from -33% to -30.8% ; the section between 5731 and 5770 m is a high value segment with $\delta^{13}C$ values ranging from -31.5% to -29.3% ; the section between 5772 and 5840 m is a mid-value segment with $\delta^{13}C$ values ranging between -32.2% and -29.8% ; the bottom of the well is a high value segment with $\delta^{13}C$ values between -31.5% and -29.3% (Fig. 6).

Table 2. Physical properties and bulk composition for the crude oil samples

Well	Sample type	Depth, m	Sand interval	Re + As	Wax	Sul	Viscosity (50 °C), $mPa \cdot s$	Density (20 °C), g/cm^3	Sat	Aro	Re	Asp	Sat/Aro
				%						%			
DH1	Oil	5726–5746	0,1	11.7	4.8	0.7	6.9	0.863					
		5756–5800	2,3	11.0	7.6	0.7	5.7	0.858	60.2	18.8	12.8	7.9	3.2
		5810–5819	4	12.2	5.25	0.9	12.47	0.882					
DH1-6-8	Oil	5726–5809	0,1,2,3						54.2	17.2	6.8	19.8	2.2
DH13	Heavy oil	5830–5858	1,2				nd	nd					
	Bitumen	5871–5886	3				nd	nd					
DH1-H4	Oil	5835–6250	1						39.9	5.8	5.4	47.5	6.9
DH1-H5	Oil	5864–6365	1						65.8	17.8	7.7	6.7	2.6
DH1-7-9	Oil	5767–5802	2,3						40.1	17.5	8.1	32.6	2.3
DH1-H18c	Oil	5981–6016	2						48.2	15.8	8.5	25.7	3.1
DH1-H17	Oil	5948–6348	1						71.4	14.9	4.7	7.0	2.6
DH20	Oil	5796–5810	4,5	13.8	5.8	0.9	15.2	0.885					
DH4	Oil	6068–6085	0,1	6.5	5.8	0.7	6.0	0.85	38.8	17.8	14.5	27.9	2.2
DH5	Oil	6076–6090	0,1	6.5	5.8	0.7	6.0	0.85					
DH6	Oil	5985–5998	0,1	8.2	5.4	0.7	6.0	0.856					
DH14	Oil	6116–6126	0,1	6.9	4.6	0.3	4.1	0.844					

Note. Re, Resin; Asp, asphaltenes; Sul, sulfur; Sat, saturated hydrocarbons; Aro, aromatic hydrocarbons; Sat/Aro, saturated hydrocarbons/aromatic hydrocarbons; nd, not determined. A blank space means there is no test data.

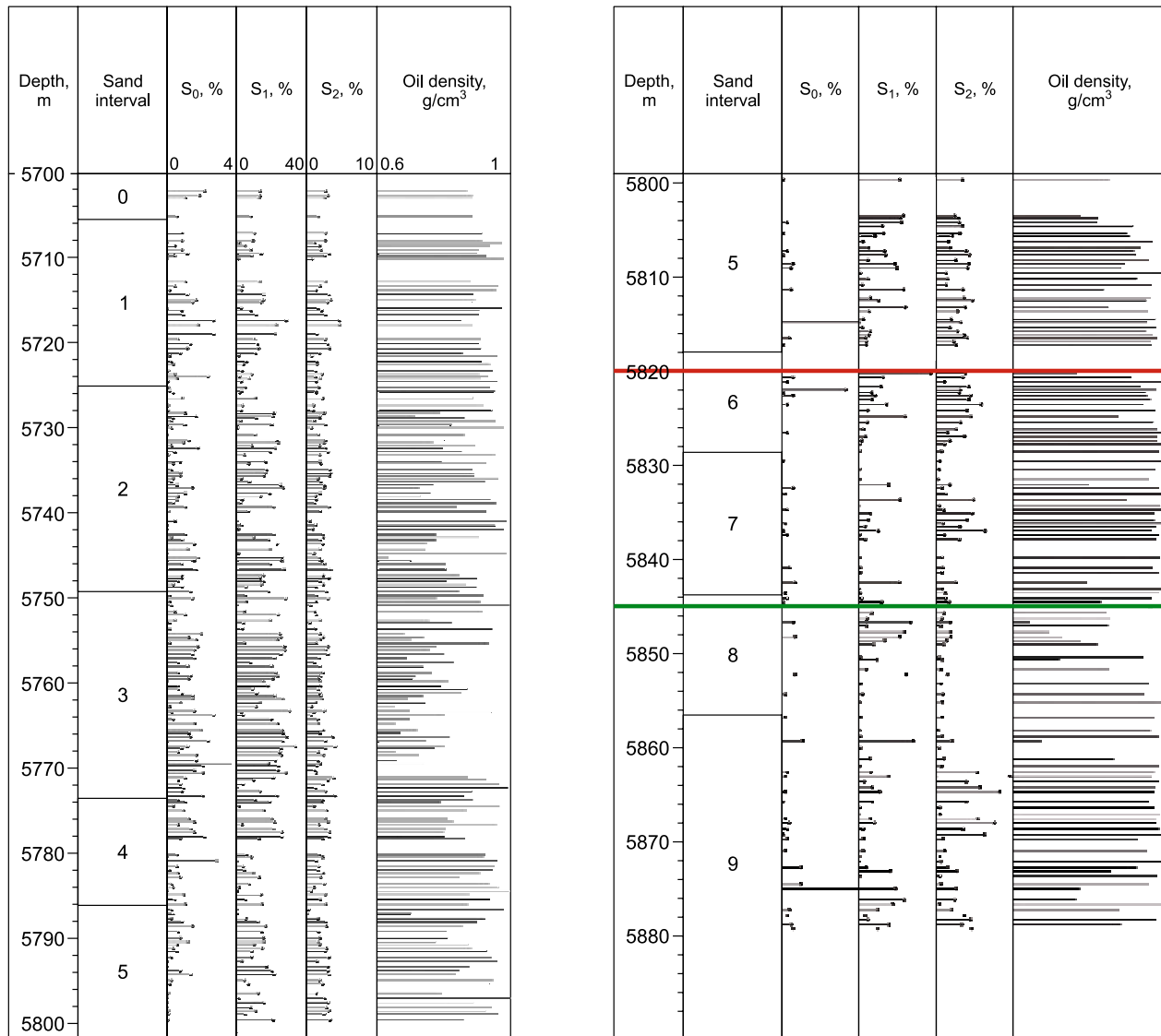


Fig. 5. Pyrolytic parameter section for the DH11 well and oil density interpretation according to the relationship shown in Fig. 4. The red line is the crude oil-water-contact interface and the green line is the heavy oil base surface. Below the depth of the green line is the formation water.

The characteristics of *n*-alkanes and light hydrocarbon composition in crude oil. The carbon chain numbers and max peak numbers range from nC_{10} to nC_{38} and 11 to 31, respectively. The value of $\sum C_{21}-/\sum C_{22}+$ varies between 0.11 and 5.18. The Pr/nC_{17} ranges primarily between 0.3 and 0.5; the abnormally high value of 0.89 in well DH20 might be related to water washing and biodegradation (Kao and Hunt, 1994; Curiale and Bromley, 1996). All the OEP and CPI values are approximately 1.0. The Ph/nC_{18} ranges between 0.35 and 0.7 and Pr/Ph is less than 1 (Table 3), which is a characteristic of marine oil (Didyk et al., 1978; Zhang and Huang, 2005).

The light hydrocarbon (C_5-C_7) compositions in the Donghe sandstone reservoir, such as the *n*-alkanes, branched alkanes, cycloalkanes and aromatics, range from 34.2 to 58.9%, 26.7 to 40.1%, 3.1 to 18.6%, and 0.1 to 16.4%, respectively (Table 4). The isopentane to *n*-pentane ratio value

(value *m*) and the isohexane to *n*-hexane ratio value (value *n*) range from 0.2 to 0.9 and 0.39 to 1.25, respectively (Table 4).

DISCUSSION

Hydrocarbon origin

There are obvious UCM drums on the saturated hydrocarbon gas chromatograph of 6 crude oil samples in the Donghetang Carboniferous Donghe sandstone reservoir (Fig. 7), which indicates that the early charging of the Donghe sandstone reservoir was subjected to biodegradation, and the complete *n*-alkane series is likely the result of late hydrocarbon charge (Volkanman et al., 1983; Curiale and Bromley, 1996; Chang et al., 2012). Residual hydrocarbons remain in the formation water layer based on pyrolysis data

Table 3. Contrast table of the geochemical parameters

Well	Sample type	Depth, m	Sand interval	Max peak	CPI	OEP	$\sum C_{21-}$ / $\sum C_{22+}$	Pr/nC ₁₇	Ph/nC ₁₈	Pr/Ph	Carbonchain range
DH1	Oil sand	5766.5	2	14	0.89	1.05	5.18	0.32	0.42	1	C ₁₂ –C ₃₄
	Oil sand	5792	3	17	0.99	1.27	2.32	0.34	0.4	0.87	C ₁₃ –C ₃₀
	Oil sand	5802	4	14	1.05	1.01	1.61	0.34	0.41	0.89	C ₁₁ –C ₃₄
	Oil sand	5811.5	4	19	1.08	1.06	1.34	0.34	0.4	0.81	C ₁₂ –C ₃₅
	Oil sand	5815.5	4	19	0.99	1	0.85	0.32	0.41	0.49	C ₁₃ –C ₃₆
	Oil sand	5825	5	21	1	1	1.08	0.31	0.38	0.82	C ₁₃ –C ₃₅
	Oil sand	5829.2	5	19	1.05	1.12	1.14	0.34	0.38	0.9	C ₁₃ –C ₃₆
	Oil sand	5837.8	5	15	1.05	0.96	2.54	0.33	0.39	0.93	C ₁₂ –C ₃₅
DH1-H17	Oil sand	5847	6	15	1.01	0.99	1.37	0.3	0.4	0.83	C ₁₃ –C ₃₄
DH20	Oil	5948–6348	1	21	1.05	1.04	1.35	0.31	0.41	0.71	C ₁₀ –C ₃₆
	Oil sand	5699.3	0	26	0.99	0.99	0.17	0.56	0.53	0.65	C ₁₅ –C ₃₈
DH1-H4	Oil sand	5704.6	0	31	1.01	1	0.11	0.89	0.69	0.57	C ₁₆ –C ₃₈
	Oil	5835–6240	1	20	0.98	1	0.85	0.24	0.42	0.32	C ₁₁ –C ₃₆
DH1-H5	Oil	5864–6365	1	11	1.08	0.87	2.05	0.31	0.4	0.81	C ₁₀ –C ₃₆
DH1-H18c	Oil	5981–6016	2	19	1.06	0.98	1.17	0.42	0.44	0.78	C ₁₄ –C ₃₆
DH1-5-5	Oil	5783–5788	1	19	1.03	1.04	2.83	0.4	0.46	0.78	C ₁₄ –C ₃₇
DH1-6-8	Oil	5726–5809	0,1,2,3	21	1.08	1.06	1.22	0.32	0.42	0.7	C ₁₀ –C ₃₆
DH1-7-9	Oil	5767–5802	2,3	18	1.09	1	1.62	0.35	0.43	0.8	C ₁₁ –C ₃₈
DH4	Oil	6068–6085	0,1	19	1.05	1.05	1.39	0.36	0.36	0.72	C ₁₅ –C ₃₆
DH6	Oil	5985–5998	0,1	19	1.03	1.04	1.16	0.4	0.46	0.78	C ₁₄ –C ₃₇

Note. Pr, pristane; Ph, phytane; $\sum C_{21-}$, the sum of the hydrocarbons with a carbon chain number lower than 21; $\sum C_{22+}$, the sum of the hydrocarbons with a carbon chain number larger than 22.

Table 4. Light hydrocarbon data and geochemical ratios calculated from gas chromatograms

Well	Sample type	Depth, m	Sand interval	a	b	c	d	k ₁	m	n
				%						
DH1-H4	Top gas	5835–6240	1	46.2	33.3	10.39	5.8	1.03	0.26	0.59
DH1-H5	Top gas	5864–6365	1	51.8	33.2	14.3	0.9	1.06	0.38	0.63
DH1-6-8	Top gas	5726–5809	1,2,3,4	50	34.1	14.8	1.1	1.08	0.37	0.67
DH1-7-9	Top gas	5767–5802	2,3	48.9	40.1	10.5	0.76	1.12	nd	0.47
DH1-H18c	Top gas	5981–6016	3	58.9	33.4	7.3	0.1	1.09	0.68	1.25
DH1-H17	Top gas	5948–6348	1	51.8	34.6	10.8	0.7	1.13	0.39	0.68
DH6	Top gas	5985–5998	1	34.2	26.7	18.6	16.4	0.88	nd	0.39
DH4	Top gas	6068–6085	1	52	33.1	3.1	0.2	1.10	0.83	0.91

Note. a, n-Alkanes; b, branched alkanes; c, cycloalkanes; d, benzene + toluene; m, isopentane/n-pentane; n, isohexane/n-hexane, k₁, (2-methylhexane + 2,3-dimethylpentane)/(3-methylhexane + 2,4-dimethylpentane); nd, not determined.

from the DH11 well (Fig. 5), which indicate that the paleo-hydrocarbon–water-contact near 5880 m and the paleo-hydrocarbon column that is between 5844 and 5880 m in the DH11 well contain data for the paleoreservoir.

There are two sets of source rocks in the Manjiaer depression: C–O₁ source rocks and O_{2–3} source rocks (Zhang et al., 2000, 2002a,b, 2011; Huang et al., 2016). The $\delta^{13}C$ values of the oil extract and bulk composition from the C–O₁ source rocks are greater than –30‰, while the O_{2–3} source rock values are lower than –31‰ (Cheng et al., 2016; Pang et al., 2016). There are two hydrocarbon charging stag-

es in the Carboniferous Donghe sandstone reservoir in the northern Tarim Basin; the early stage occurred during the Permian to the Triassic and the later stage occurred in the Neogene (Zhu et al., 2013a,b).

The paleohydrocarbon column $\delta^{13}C$ values in the section from 5844 to 5856 m indicate that they originated from the C–O₁ source rocks (Fig. 8). The $\delta^{13}C$ bulk composition values from the DH11 rock extracts indicate that the present-day crude oil in the section from 5700 to 5840 m is primarily derived from the O_{2–3} source rocks and mixed with C–O₁ source rock hydrocarbons. Zhu et al. (2013a,b), Cheng et al.

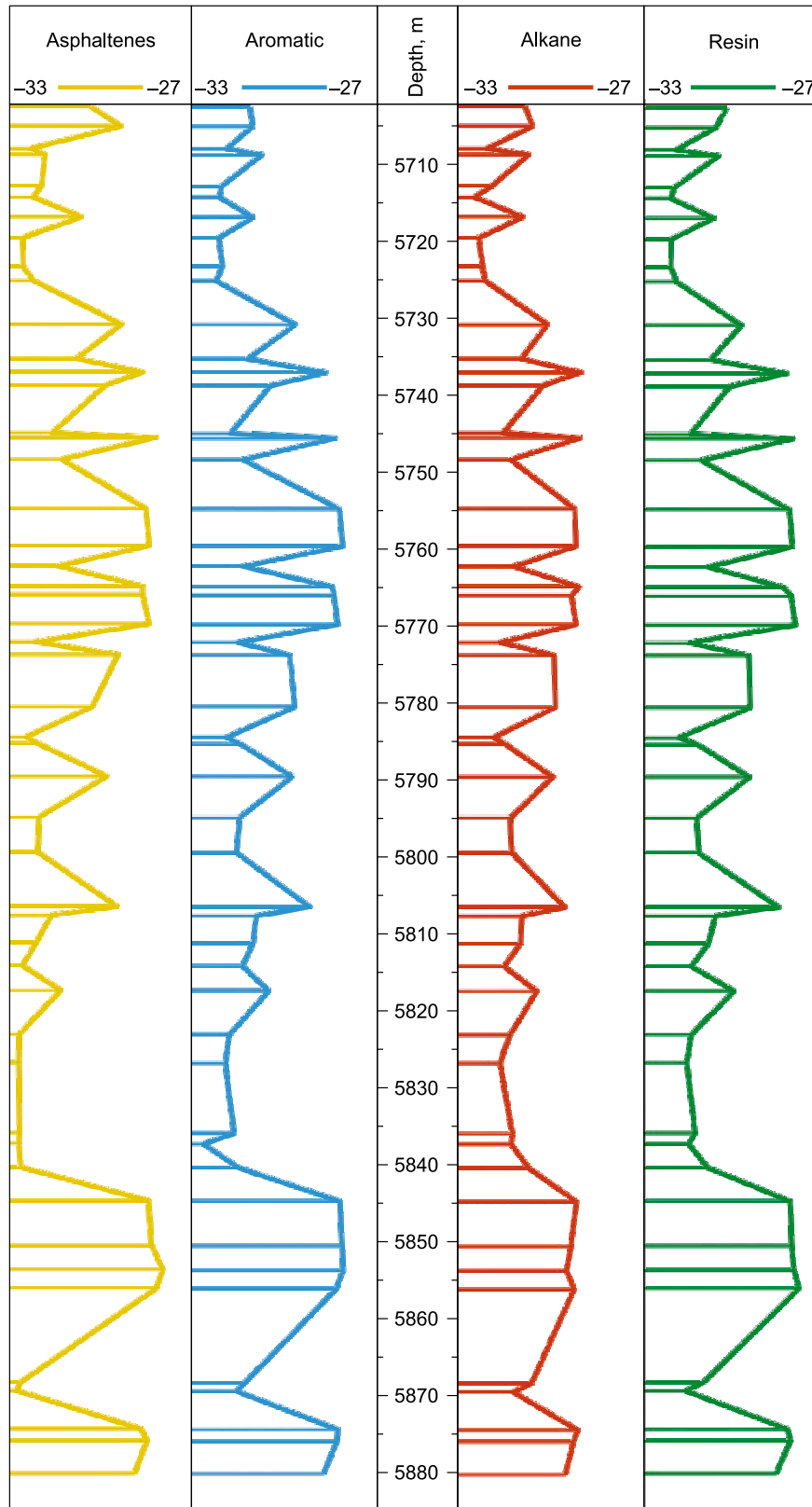


Fig. 6. The bulk component $\delta^{13}\text{C}$ values of the rock extracts from the DH11 well.

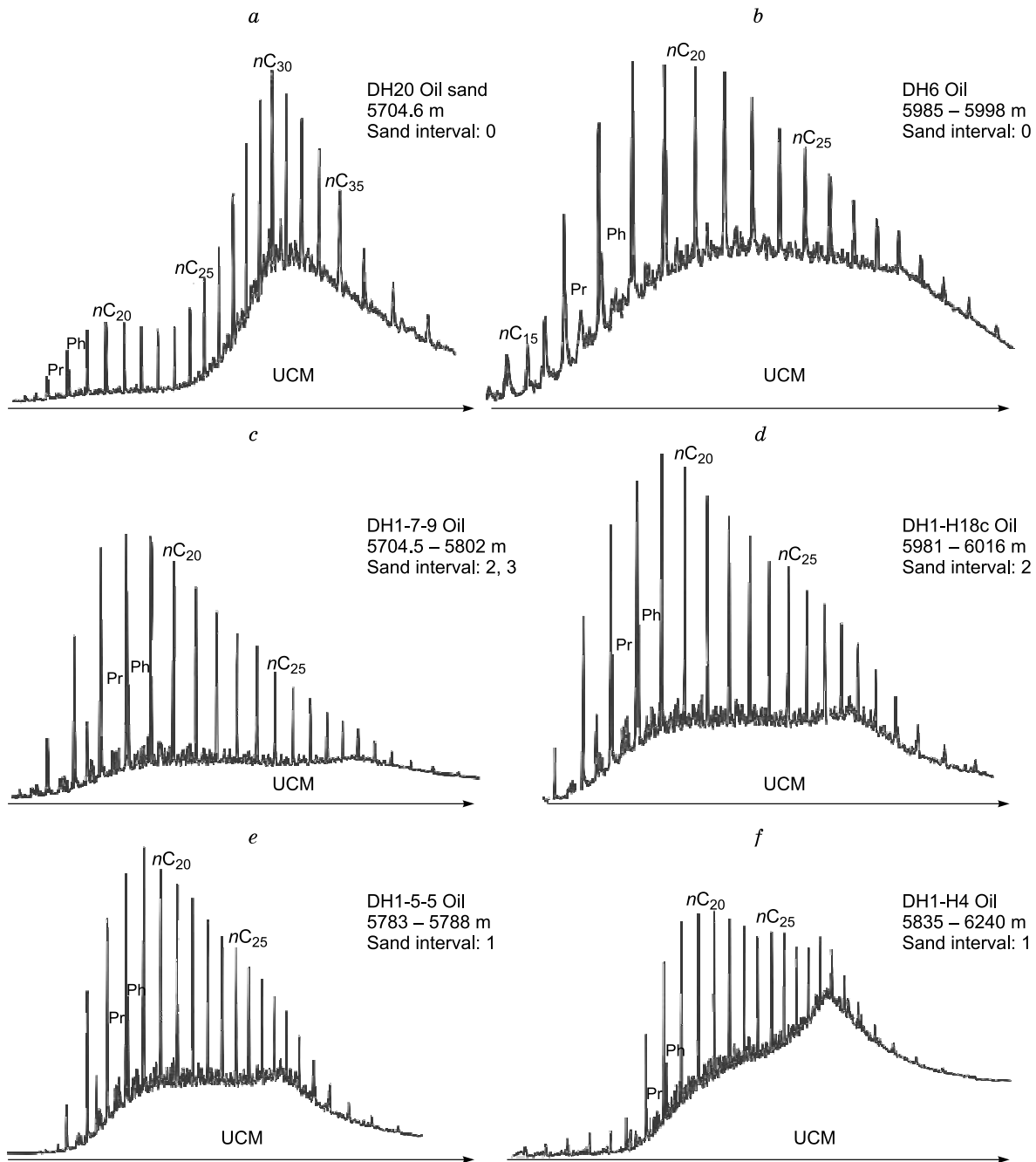


Fig. 7. Representative *n*-alkane hydrocarbon fraction gas chromatograms. The samples from the DH1 well at a depth of 5825 m and the DH11 well at a depth of 5737.3 m are from whole oil gas chromatograms, whereas the others are saturated hydrocarbon fraction gas chromatograms. Pr, pristane; Ph, phytane; *n*, normal alkanes; *C_j*, carbon number.

(2016) and Ni et al. (2016) proposed that the hydrocarbon generation peak was derived from the ϵ source rocks in the late Silurian and experienced strong biodegradation in the Devonian, which indicates that the Carboniferous Donghe sandstone cannot trap hydrocarbons derived from the ϵ source rocks. Hence, the paleoreservoir hydrocarbons charged in the Permian to the Triassic originated from the O_1 source rocks and the present-day-reservoir hydrocarbons charged in the Neogene originated from the O_{2-3} source rocks.

Secondary alteration

Water washing and biodegradation. Water washing significantly reduces the crude oil aromatic component, especially the light aromatics such as benzene and toluene (Palmer, 1993), and C_4 – C_7 paraffins are easily dissolved in water and lost by washing (Lafargue and Barker, 1988). The low toluene and benzene values below 1% (Table 4) in the crude oil samples from the six wells were caused by water washing.

The UCM drum on the alkaline gas chromatograph is widely distributed in the sand intervals from 0 to 3 (Fig. 7) and heavy oil is distributed throughout the entire hydrocarbon column in the DH11 well (Fig. 5), which all indicate the occurrence of biodegradation throughout the entire reservoir.

The Donghe sandstone was partially uplifted to the surface due to compressional forces during the Permian to the Triassic (An et al., 2009). Due to long-term exposure at the surface, the atmospheric fresh water became connected to the bottom water of the Donghe sandstone reservoir through an unconformity surface and fault, which both formed in the Permian–Triassic. Lafargue and Barker (1988) proposed that the biodegradation and water washing could have occurred simultaneously if the temperature was below 80 °C. The homogenization temperature of the Donghe sandstone fluid inclusions in Well DH11 range from 65.8 to 76.5 °C (Zhang et al., 2012), which indicates that the Donghe sandstone reservoirs were suitable for both biodegradation and water washing during hydrocarbon accumulation.

In the early stages of hydrocarbon migration and accumulation, the active bottom water was likely transported into the presence of oxygen-enriched bacteria, leading to hydrocarbon biodegradation and thickening (Fig. 9). With the gradual accumulation of hydrocarbons, the reservoirs far from the oil-water contact were under hypoxia conditions, and the aerobic bacteria dissipated and were gradually re-

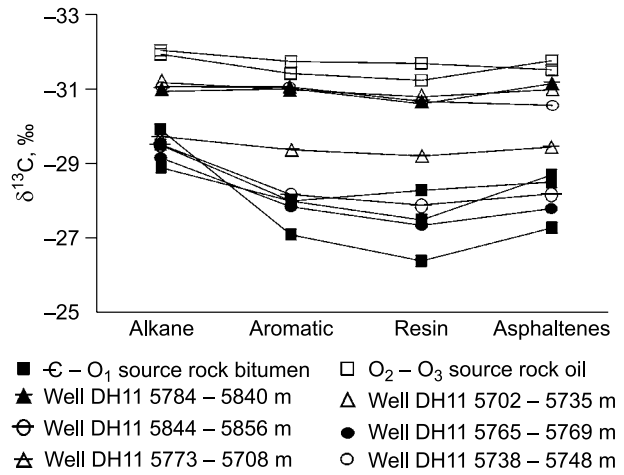


Fig. 8. The $\delta^{13}\text{C}$ values of the bulk composition distribution for the different source rocks (data from (Cheng et al., 2016)). The of bulk composition $\delta^{13}\text{C}$ values are from rock extracts in the DH11 well.

placed by anaerobic bacteria. The anaerobic bacteria could only consume the crude oil oxidative degradation products via BSR (Machel et al., 1995). The BSR resulted in high sulfur reduction that produced H_2S , pyrite and other sulfides and simultaneously precipitated asphaltenes (Means and Hubbard, 1987). Additionally, BSR was the primary reason pyrites were accompanied by heavy oil and asphaltenes in

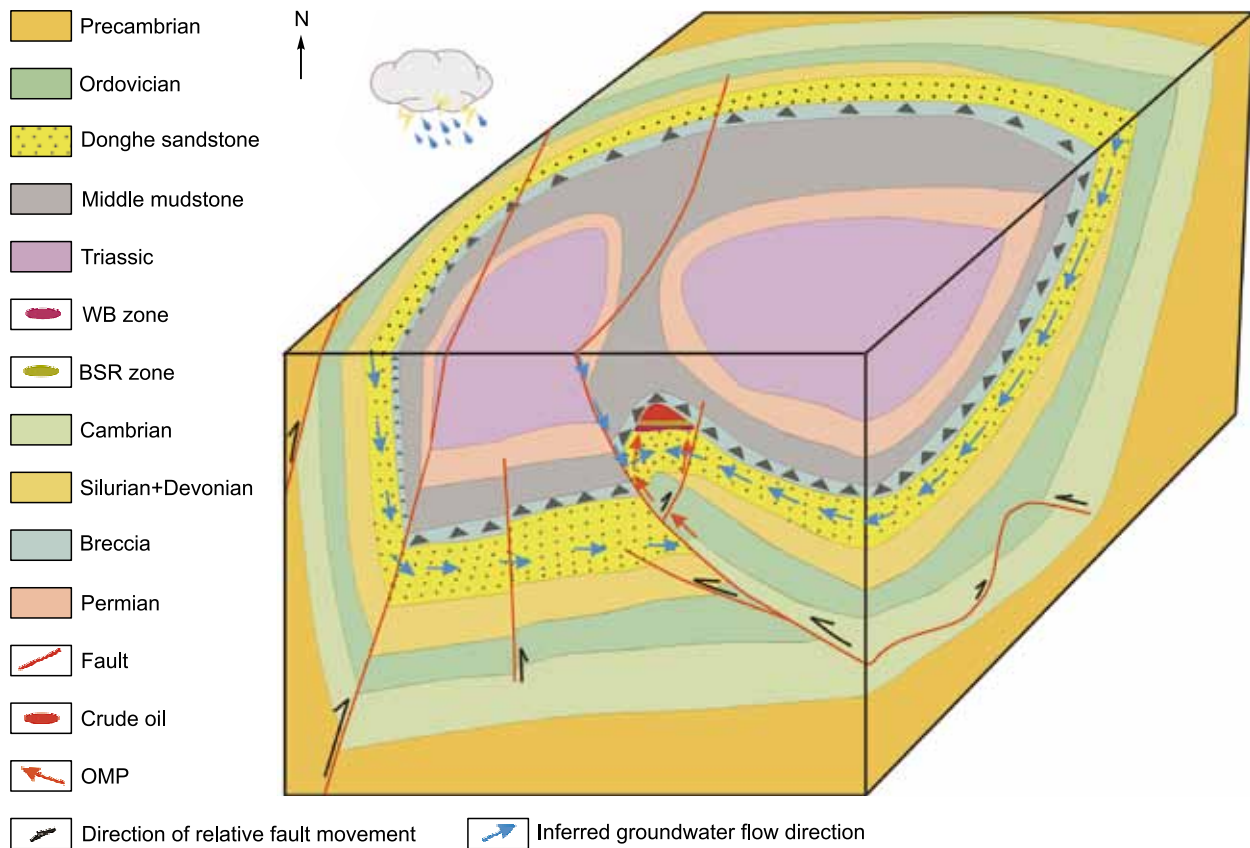


Fig. 9. The model of oil accumulation and biodegradation in the late Permian–Early Triassic of the Donghe sandstone reservoir, Donghetang area, not to scale. BSR, bacteria sulfate reduction; WB, water washing and biodegradation; OMP, oil migration pathway.

the core description. After the production of bacteria was consumed, the BSR by the anaerobic bacteria terminated.

Therefore, the hydrocarbon accumulation in the paleoreservoir from the Permian to the Triassic was a continuous process of oil and gas migration accompanied by water washing, biodegradation and BSR (Fig. 9). These were also the primary reasons for the presence of biodegradation and heavy oil distribution throughout the entire Donghe sandstone reservoir section (Figs. 5 and 7).

Gas washing and evaporative fractionation. Gas washing and evaporative fractionation are the processes of condensate oil and light oil formation due to increased natural gas generation from highly mature source rocks migrating into the reservoirs. The gas dissolves and alters the crude oil forming a light fraction hydrocarbon with a moderate molecular weight under high temperature and pressure reservoir conditions. The hydrocarbons migrated along faults and unconformities to the overlying reservoir under fluid pressure balance failure conditions, which indicates that condensate oil and gas can originate directly from the physical frac-

tionation of crude oil (Price et al., 1983; Thompson, 1987, 1988; Zhang et al., 2000).

Kissin (1987) proposed that there is a linear relationship between the logarithm of n -alkane molarity and the corresponding carbon number in the unaltered crude oil by studying 50 crude oil samples:

$$\lg [MC(n)] = a \cdot n + \lg(A),$$

where $MC(n)$ is the n -alkane molarity, n is the n -alkane carbon number a is the slope of the linear fitting line, and A is the normalized factor.

The n -alkane molarity in crude oil will change as different secondary alteration processes occur. The molarity of n -alkanes lighter than nC_{13} decreases as gas washing occurs. The molarity of n -alkanes lighter than nC_{15} increases as gas intrusion occurs. The n -alkane molarity decreases between nC_{15} and nC_{25} as evaporative fractionation occurs (Meulbroek et al., 1998). Losh et al. (2002) proposed a method to calculate the loss of n -alkanes in crude oil using the oil compositional changes and defined Q as the quantitative evalua-

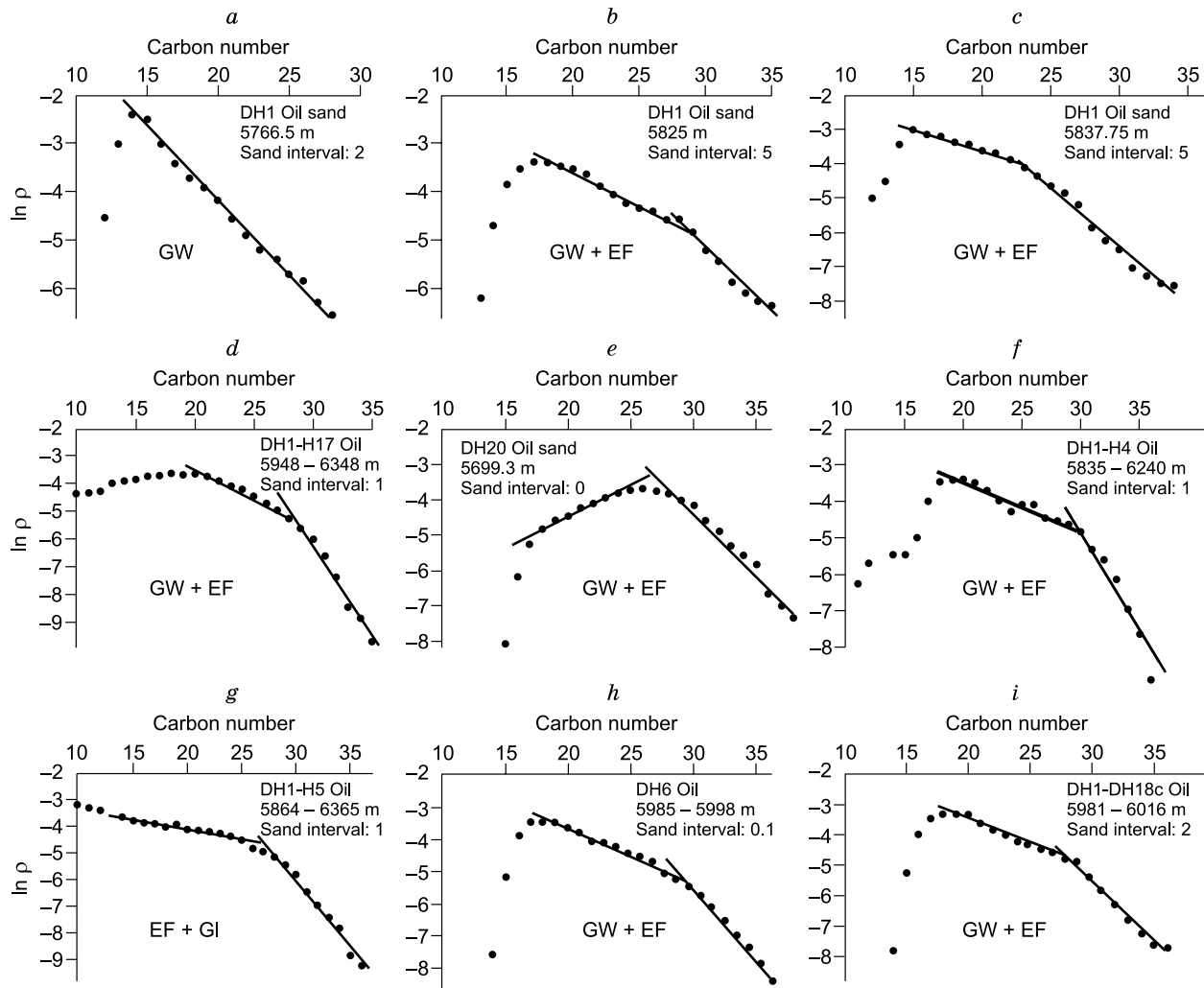


Fig. 10. Representative curve of the n -alkanes molar concentration in the study area. The logarithm of the n -alkane mole fractions. GW, gas washing; EF, evaporative fractionation; GI, gas intrusion.

Table 5. Secondary alteration type origin from gaseous hydrocarbon charge in the Donghe sandstone reservoir

Well	Depth, m	Sample type	Sand interval	Slope	R^2	Turnoff carbon number	Secondary alteration type	Q, %
DH1	5766.5	Oil sand	2	−0.32	0.9929	15	GW	86.6
	5792	Oil sand	3	/	/	24	GW + EF	94.1
	5802	Oil sand	4	/	/	25	GW + EF	86.7
	5811.5	Oil sand	4	/	/	30	GW + EF	85.4
	5815.5	Oil sand	4	−0.1696	0.9684	19	GW	89.2
	5825	Oil sand	5	/	/	29	GW + EF	90.4
	5829.15	Oil sand	5	−0.16	0.9534	15	GW	85.8
	5837.74	Oil sand	5	/	/	27	GW + EF	95.7
	5847	Oil sand	6	−0.1419	0.9798	15	GW	84.5
DH1-H17	5948–6348	Oil	1	/	/	29	GW + EF	80.4
DH20	5699.3	Oil sand	0	/	/	28	GW + EF	98.6
	5704.6	Oil sand	0	/	/	31	GW + EF	93.3
DH1-H4	5835–6240	Oil	1	/	/	30	GW + EF	94.7
DH1-H5	5864–6365	Oil	1	/	/	26	GI + EF	/
DH1-H18c	5981–6016	Oil	2	/	/	29	GW + EF	91.8
DH1-5-5	5783–5788	Oil	1	/	/	32	GW + EF	95.2
DH1-6-8	5726–5809	Oil	0,1,2,3	/	/	28	GW + EF	82.9
DH1-7-9	5767.5–5802	Oil	2,3	/	/	28	GW + EF	96.7
DH4	6068–6085	Oil	0,1	−0.2538	0.9911	19	GW	94.8
DH6	5985–5998	Oil	0,1	/	/	30	GW + EF	90.8

Note. R^2 , correlation coefficient; Turnoff carbon number: the hydrocarbons lost below a certain carbon chain number due to gas washing and/or evaporative fractionation; Q, amount of n -alkane losses; GW, gas washing; EF, evaporative fractionation; GI, gas intrusion. The well location is shown in Fig. 1.

tion standard for the gas-washing strength; more detailed information is reported in Losh et al. (2002).

Figure 10 shows the molarity curves for n -alkanes in 9 wells drilled in the Donghe sandstone reservoir, Donghetang area, indicating that gas washing and evaporative fractionation widely affected this reservoir. The loss of n -alkanes occurs before nC_{18} exceeds 80% due to gas washing and evaporation fractionation alteration, and these alterations have nearly consumed all the n -alkanes before C_{28} in the crude oil for sand interval 0 in the DH20 well (Table 5).

In the condensate hydrocarbon formation process from gas washing and evaporative fractionation migration upwards, the dissolution properties of the gaseous hydrocarbons will vary due to temperature and pressure changes, which leads to exsolution, an increase in wax content and an enrichment of n -alkanes with a medium molecular weight of nC_{16} to nC_{30} (Price et al., 1983; Zhang, 2000). The Donghe sandstone reservoirs with high n -alkane carbon numbers, high wax content, light oil and condensate oil are the result of combined gas washing and evaporative fractionation.

The n -alkanes molar concentration curve in the DH1-H5 well shows that the molar concentrations of n -alkanes lighter than nC_{15} increases (Fig. 10g), which indicates that the DH1-H5 well experienced gas intrusion. Gas intrusion might arise when interlayer barriers exist, which can lead to gaseous hydrocarbons that cannot migrate and accumulate in the local trap.

Natural gas origin

Hydrocarbon gas. Wang et al. (2008) proposed that when i/nC_4 is less than 0.9, gas could be formed under three different conditions. Gas can form due to mixed liquid hydrocarbon cracking and kerogen degradation in a closed system, hydrocarbon cracking, or kerogen degradation for cases in which i/nC_5 is less than 0.6, ranging from 0.6 to 0.85 or greater than 0.85, respectively. Since i/nC_4 ranges between 0.26 and 0.83 and i/nC_5 ranges between 0.39 and 1.25 in the Donghe sandstone reservoir (Table 4), the gases in this reservoir are derived from both kerogen degradation and liquid hydrocarbon cracking.

Mango (1987, 1990) suggested that the K_1 values, defined by (2-methylhexane + 2,3-dimethylpentane)/(3-methylhexane + 2,4-dimethylpentane), of hydrocarbons from the same source are basically consistent. The K_1 gas value in the Donghe sandstone reservoir is relatively consistent, ranging from 0.88 to 1.13 (Table 4), indicating that the gas formed by kerogen degradation and oil cracking originated from the same source rocks. Lu et al. (2007) suggested that the gas is the product of the O_{2-3} hydrocarbon mature source rocks in the Manjiaer depression by calculating the gas source rock maturity using methane carbon isotopes.

Nonhydrocarbon gas. Organic CO_2 is characterized by low $\delta^{13}C$ values that are less than -10% , whereas inorganic CO_2 has high $\delta^{13}C$ values that are greater than -8% , and volcanic CO_2 ranges from -8.4 to -3.4% (Dai et al., 1996).

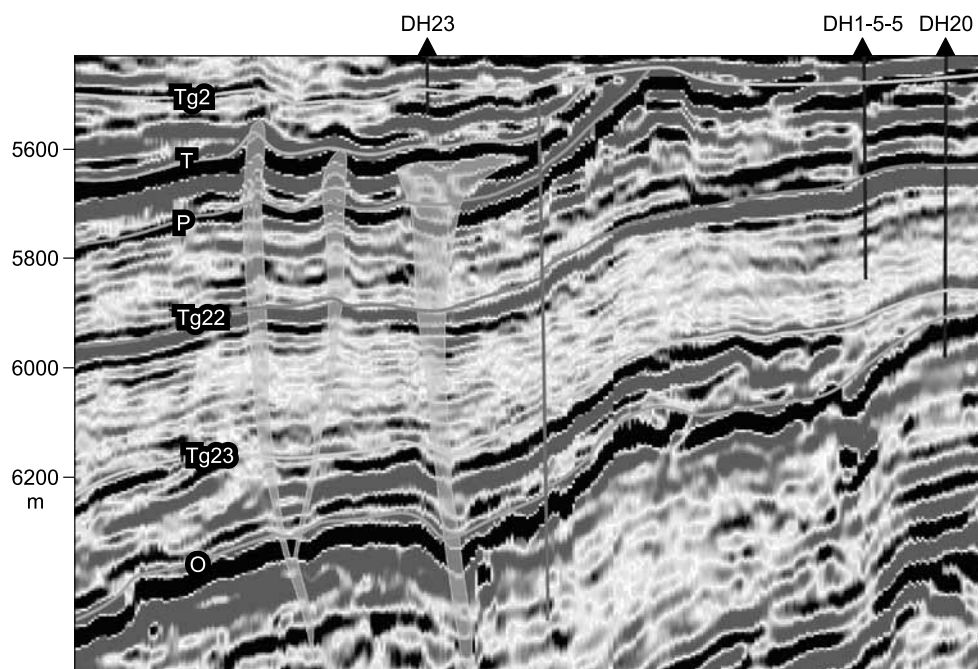


Fig. 11. The characteristics of volcanic vents and rocks in the seismic profile, Donghetang area. T is the Triassic strata top surface. The well location is shown in Fig. 1. Tg2, Triassic system top surface; T, Triassic system bottom surface; P, Permian system bottom surface; Tg22, Donghe sandstone top surface; Tg23, Donghe sandstone bottom surface; O, Ordovician system top surface.

The $\delta^{13}\text{C}$ value of CO_2 in the Donghe sandstone for the DH1-6-8 and DH11 wells was -4.6 and -7.55% , respectively (Wang et al., 2001), which indicates that the CO_2 has a volcanic origin. The $\delta^{15}\text{N}$ value of N_2 in the Donghe sandstone for the DH1-6-8 well was 14.6% (Liu et al., 2007), and this value far exceeds that formed by organic nitrogen through thermal ammoniation when the kerogen maturity ranges from -10 to -2% (Zhu et al., 2000), which suggests that N_2 should have an inorganic origin.

There was strong volcanic activity during the Permian to the Early Triassic in the western Tabei Uplift (Liu et al., 2012). The seismic profile across the DH1 oilfield shows volcanic vents and seismic reflection characteristics such as mounds, strong chaotic amplitude seismic reflections, and seismic events that show upwarps and downwarps in the profile (Fig. 11). A thick tuff was drilled by the DH4, DH5, and DH6 wells, which indicated the occurrence of volcanic activity. The combined $\delta^{13}\text{C}$ values of CO_2 and the $\delta^{15}\text{N}$ values of N_2 in the Donghe sandstone reservoir suggests that CO_2 and N_2 originated from volcanic activity during the Permian to the Early Triassic.

CONCLUSIONS

There are at least two hydrocarbon charging stages in the study area. The paleoreservoirs that formed in the early stage originated from the O_1 source rocks. The present-day reservoirs that formed in the later stage originated from the O_{2-3} source rocks. Hydrocarbon gas formed due to liquid

hydrocarbon cracking and kerogen degradation, while non-hydrocarbon gas originated from volcanic degassing.

The paleoreservoir formed during the Permian to the Triassic and experienced water washing and biodegradation during the continuous hydrocarbon accumulation, while meteoric fresh water flowed into the Carboniferous sandstone reservoirs through faults and unconformity surfaces. The processes of continuous hydrocarbon accumulation, water washing, biodegradation, and BSR occurred simultaneously. H_2S , pyrite and asphaltenes formed during bacteria-sulfate reduction.

The original reservoir experienced gas washing and evaporative fractionation by natural gas that originated from the O_{2-3} source rocks. This formed a symbiosis between heavy oil, crude oil, light oil, condensate oil and natural gas in one Carboniferous Donghe sandstone reservoir and, concurrently, a high wax content, and high carbon number hydrocarbons in a secondary reservoir.

The authors are thankful for permission to publish this paper and acknowledgment for data contribution and sample collection from the Research Institute of Petroleum Exploration and Development in Tarim Oilfield Company, PetroChina. This research was funded by the National Science and Technology Major Project (No. 2017ZX05001) in China. We are grateful to editors and anonymous reviewers for very constructive and useful comments.

REFERENCES

- An, H.Y., Li, H.Y., Wang, J.Z., Du, X.F., 2009. Tectonic evolution and its controlling on oil and gas accumulation in the Northern Tarim

- Basin [in Chinese with English abstract]. *Geotectonica et Metallogenia* 33 (1), 142–147.
- Chang, X.C., Wang, T.G., Li, Q.M., Cheng, B., Zhang, L.P., 2012. Maturity assessment of severely biodegraded marine oils from the Halahatang depression in Tarim Basin. *Energy Explor. Exploit.* 30 (2), 331–350.
- Chang, X.C., Wang, T.G., Li, Q.M., Cheng, B., Tao, X.W., 2013. Geochemistry and possible origin of petroleum in Palaeozoic reservoirs from Halahatang Depression. *J. Asian Earth Sci.* 47, 129–141.
- Cheng, B., Wang, T.G., Chen, Z.H., Chang, X.C., Yang, F.L., 2016. Biodegradation and possible source of Silurian and Carboniferous reservoir bitumens from Halahatang sub-depression, Tarim Basin, NW China. *Mar. Pet. Geol.* 78, 236–246.
- Cheng, H.Y., Li, J.H., Zhao, X., 2009. The structural styles of different structural layers in the western part of north Tarim Uplift and Their genetic mechanisms [in Chinese with English abstract]. *Geol. J. China Univ.* 15 (4), 529–326.
- Curiale, J.A., Bromley, B.W., 1996. Migration induced compositional changes in oils and condensates of a single field. *Org. Geochem.* 24, 1097–1113.
- Dai, J.X., Song, Y., Dai, C.S., Wang, D.R., 1996. Geochemistry and accumulation of carbon dioxide gases in China. *AAPG* 80 (10), 1615–1626.
- Didyk, B.M., Simoneit, B.R.T., Brassell, S.C., Eglinton, G., 1978. Organic geochemical indicators of palaeoenvironmental conditions of sedimentation. *Nature* 272, 216–222.
- Dzou, L.I.P., Hughes, W.B., 1993. Geochemistry of oils and condensates, K. Field, offshore Taiwan: A case study in migration fractionation. *Org. Geochem.* 20 (4), 437–462.
- Guo, X.W., Liu, K.Y., Jia, C.Z., Song, Y., Zhao, M.J., Zhuo, Q.H., Lu, X.S., 2016. Effects of tectonic compression on petroleum accumulation in the Kelasu Thrust Belt of the Kuqa Sub-basin, Tarim Basin, NW China. *Org. Geochem.* 101, 22–37.
- Huang, H.P., Zhang, S.C., Su, J., 2016. Palaeozoic oil-source correlation in the Tarim Basin, NW China: A review. *Org. Geochem.* 94, 32–36.
- Jia, L., Cai, C., Yang, H., Li, H., Wang, T., Zhang, B., Jiang, L., 2015. Thermochemical and bacterial sulfate reduction in the Cambrian and Lower Ordovician carbonates in the Tazhong Area, Tarim Basin, NW China: evidence from fluid inclusion, C, S, and Sr isotopic data. *Geofluids* 15, 421–437.
- Kao, C.S., Hunt, J.R., 1994. A plug flow model of liquid infiltration into dry soils. *Geophys. Union Hydrol. Days* 14, 183–193.
- Kissin, Y., 1987. Catagenesis and composition of petroleum: Origin of *n*-alkanes and isoalkanes in petroleum crudes. *Geochim. Cosmochim. Acta* 51 (9), 2445–2457.
- Lafargue, E., Barker, C., 1988. Effect of water washing on crude oil composition. *AAPG* 72, 263–276.
- Li, G.D., Liang, D.G., Jia, C.Z., Basharin, A.K., Belyaev, S.Y., Fradkin, G.S., 1998. Geology and petroleum potential of the Tarim platform. *Geologiya i Geofizika (Russian Geology and Geophysics)* 39 (10), 1402–1415.
- Li, W.L., Xu, H.M., Niu, Y.J., Wang, C., Gao, S.Y., 2016a. Sand body types of clastic shore deposits with delta backgrounds and their control over reservoir quality. *Arab. J. Geosci.* 9, 247. DOI: 10.1007/s12517-015-2276-7.
- Li, Z.X., Xu, Z.M., Wang, Z.M., Chen, Yu., Xiao, Zh., 2016b. Geochemical characteristics of crude oil and oil-source correlation in Halahatang sag [in Chinese with English abstract]. *Xinjiang Pet. Geol.* 37 (6), 667–673.
- Liu, Q.Y., Dai, J.X., Liu, W.H., Qin, S.F., Zhang, D.W., 2007. Geochemical characteristics and genesis of nitrogen in natural gas from Tarim Basin [in Chinese with English abstract]. *Oil Gas Geol.* 28 (1), 12–17.
- Liu, Y.L., Huang, Z.B., Wu, G.Y., Wu, G.Y., Zheng, D.M., 2012. ⁴⁰Ar–³⁹Ar geochronology and geochemistry of the volcanic rocks from the west segment of Tabei Uplift, Tarim Basin [in Chinese with English abstract]. *Acta Petrol. Sinica* 28 (8), 2423–2434.
- Losh, S., Cathles, L., Meulbroek, P., 2002. Gas washing of oil along a regional transect offshore Louisiana. *Org. Geochem.* 33, 655–663.
- Lu, Y.H., Xiao, Z.R., Gu, Q.Y., Zhang, Q.C., 2007. Geochemical characteristics and accumulation of marine oil and gas around Halahatang depression, Tarim basin, China [in Chinese]. *Sci. China (Ser. D)* 51 (Suppl.), 167–176.
- Mango, F.D., 1987. An invariance in the isoheptanes of petroleum. *Science* 273, 514–517.
- Mango, F.D., 1990. The origin of light cycloalkanes in petroleum. *Geochim. Cosmochim. Acta* 54, 23–27.
- Machel, H.G., Krouse, H.R., Saasen, R., 1995. Products and distinguishing criteria of bacterial and thermochemical sulfate reduction. *Appl. Geochem.* 373–389.
- Matyasik, I., Steczko, A., Philp, R.P., 2000. Biodegradation and migrational fractionation of oils from the Eastern Carpathians, Poland. *Org. Geochem.* 31, 1509–1523.
- Masterson, W.D., Dzou, L.I.P., Holba, A.G., Fincannon, A.L., Ellis, L., 2001. Evidence for biodegradation and evaporative fractionation in West Sak, Kuparuk and Prudhoe Bay field areas, North Slope, Alaska. *Org. Geochem.* 32: 411–441.
- Means, J.L., Hubbard, N.J., 1987. Short-chain aliphatic acid anions in deep subsurface brines: A review of their origin, occurrence, properties, and importance and new data on their distribution and geochemical implications in Palo Duro Basin, Texas. *Org. Geochem.* 11, 177–191.
- Meulbroek, P., Gathles, III. L., Whelan, J., 1998. Phase fractionation at South Eugene Island Block 330. *Org. Geochem.* 29 (1–3), 223–239.
- Ni, Z.Y., Wang, T.G., Li, M.J., Fang, R.H., Li, Q.M., Tao, X.W., 2016. An examination of the fluid inclusion of the well RP3-1 at the Halahatang Sag in Tarim Basin, northwest China: Implications for hydrocarbon charging time and fluid evolution. *J. Pet. Sci. Eng.* 146, 326–339.
- Palmer, S.E., 1984. Effect of biodegradation and water washing on C₁₅+ hydrocarbon fraction of crude oils from northwest Palawan, Philippines. *AAPG Bull.* 68, 137–149.
- Pang, X.Q., Chen, J.Q., Li, S.M., Chen, J.F., Wang, Y.X., Pang, H., 2016. Evaluation method and application of the relative contribution of marine hydrocarbon source rocks in the Tarim Basin: A case study from the Tazhong area. *Mar. Pet. Geol.* 77, 1–18.
- Price, L.I.P., Wenger, L.M., Ging, T., Blount, C.W., 1983. Solubility of crude oil in methane as a function of pressure and temperature. *Org. Geochem.* 4, 201–221.
- Song, D.F., Wang, T.G., Deng, W.L., Shi, S.B., 2016. Application of light hydrocarbons (C5–C7) in Paleozoic marine petroleum of the Tarim Basin, NW China. *J. Pet. Sci. Eng.* 140, 57–63.
- Tang, L.J., Jin, Z.J., Zhang, Y.W., Lu, K.Z., 1999. Negative inversion structures and geological significance of Northern Uplift, the Tarim Basin, NW China [in Chinese with English abstract]. *Geoscience* 13 (1), 93–98.
- Tao, X.W., Zhang, Y.J., Duan, S.F., Zhang, L., 2015. Crude oil accumulation process and causes of highly variable oil density in Halahatang oilfield, Tarim Basin [in Chinese with English abstract]. *Acta Petrol. Sinica* 36 (4), 405–415.
- Thompson, K.F.M., 1987. Fractionated aromatic petroleum and the generation of gas-condensates. *Org. Geochem.* 11 (6), 573–590.
- Thompson, K.F.M., 1988. Gas-condensate migration and the petroleum fractionation in deltaic system. *Mar. Pet. Geol.* 5 (4), 237–245.
- Tian, Y., Yang, C.P., Liao, Z.W., Zhang, H.Z., 2012. Geochemical quantification of mixed marine oils from Tazhong area of Tarim Basin, NW China. *J. Pet. Sci. Eng.* 90, 96–106.
- Volkanman, J.K., Alexander, R., Kagi, R.I., Woodhouse, G.W., 1983. Demethylated hopanes in crude oil and their applications in petroleum geochemistry. *Geochim. Cosmochim. Acta* 47, 785–794.

- Wang, G.A., Shen, J.Z., Ji, M.Y., 2001. Carbon isotopic composition and origin of carbon dioxide in natural gases in northern and central Tarim Basin [in Chinese with English abstract]. *Geol. Geochem.* 29 (4), 36–39.
- Wang, G.L., Xue, Y.C., Wang, D.W., Shi, S.B., Grice, K., Greenwood, P.F., 2016. Biodegradation and water washing within a series of petroleum reservoirs of the Panyu Oil Field. *Org. Geochem.* 96, 65–76.
- Wang, Y.P., Zhao, C.Y., Wang, Z.Y., Wang, H.J., Zou, Y.R., Liu, J.Z., 2008. Identification of marine natural gases with different origin sources. *Sci. China (Ser. D)* 51 (Suppl. 1), 148–164.
- Zhang, B., Zhu, G.Y., Su, J., Lu, Y.H., 2012. Origin and distribution of hydrocarbon in Donghe Oilfield, west Tabei Uplift, Tarim basin [in Chinese with English abstract]. *Earth Sci. Front.* 19 (4), 276–283.
- Zhang, S.C., 2000. The migration fractionation: An important mechanism in the formation of condensate and waxy oil. *Chin. Sci. Bull.* 45 (14), 1341–1344.
- Zhang, S.C., Huang, H.P., 2005. Geochemistry of Palaeozoic marine petroleum from the Tarim Basin, NW China. Pt. 1: Oil family classification. *Org. Geochem.* 36 (8), 1204–1214.
- Zhang, S.C., Hanson, D.G., Liang, D.G., Chang, E., Fago, F., Hanson, A.D., 2000. Paleozoic oil source rock correlation in the Tarim basin, NW China. *Org. Geochem.* 31 (4), 273–286.
- Zhang, S.C., Liang, D.G., Li, M.W., Xiao, Z.Y., He, Z.F., 2002a. Molecular fossils and oil-source rock correlations in the Tarim Basin, NW China. *Chin. Sci. Bull.* 47 (Suppl.), 20–27.
- Zhang, S.C., Moldowan, J.M., Li, M.W., Bian, L.Z., Zhang, B.M., He, Z.F., Wang, D.R., 2002b. The abnormal distribution of the molecular fossils in the pre-Cambrian and Cambrian: Its biological significance. *Sci. China (Ser. D)* 45 (3), 193–200.
- Zhang, S.C., Zhang, B.M., Li, B.L., Zhu, G.Y., Su, J., Wang, X.M., 2011. History of hydrocarbon accumulations spanning important tectonic phases in marine sedimentary basins of China: Taking the Tarim Basin as an example. *Pet. Explor. Develop.* 38 (1), 1–15.
- Zhu, Y., Shi, B., Fang, C., 2000. The isotopic compositions of molecular nitrogen: implication on their origins in natural gas accumulations. *Chem. Geol.* 164, 321–330.
- Zhu, G.Y., Zhang, S.C., Su, J., Zhang, B., Yang, H.J., Zhu, Y.F., Gu, L.J., 2013a. Alteration and multi-stage accumulation of oil and gas in the Ordovician of the Tabei Uplift, Tarim Basin, NW China: Implication for genetic origin of the diverse hydrocarbons. *Mar. Pet. Geol.* 46, 234–250.
- Zhu, G.Y., Zhang, S.C., Su, J., Meng, S.C., Yang, H.J., Hu, J.F., Zhu, Y.F., 2013b. Secondary accumulation of hydrocarbons in Carboniferous reservoirs in the northern Tarim Basin, China. *J. Pet. Sci. Eng.* 102, 10–26.

Editorial responsibility: A.E. Kontorovich